

Electronic Supplementary Information

Using L-STM to directly visualize enzymatic self-assembly/disassembly of nanofibers

Zhen Zheng,^{‡a,b} Jihao Wang,^{‡a,c} Peiyao Chen,^{a,b} Maolin Xie,^d Lei Zhang,^a Yubin Hou,^a Xin Zhang,^a
Jun Jiang,^{c,d} Junfeng Wang,^{*a} Qingyou Lu,^{*a,b,e} and Gaolin Liang^{*a,b}

^aHigh Magnetic Field Laboratory, Hefei Science Center, Chinese Academy of Sciences and University of Science and Technology of China, Hefei, Anhui, China.

^bCAS Key Laboratory of Soft Matter Chemistry, Department of Chemistry, University of Science and Technology of China, Hefei, Anhui 230026, China

^cHefei National Laboratory for Physical Sciences at Microscale, University of Science and Technology of China, Hefei, Anhui 230026, China

^dDepartment of Chemical Physics, University of Science and Technology of China, Hefei, Anhui 230026, China

^eCollaborative Innovation Center of Advanced Microstructures, Nanjing University, Nanjing, Jiangsu 210093, China

[‡]These authors contributed equally to this work.

*Corresponding authors: junfeng@hmfl.ac.cn (J-F. W.); qxl@ustc.edu.cn (Q. L.); gliang@ustc.edu.cn (G. L.).

Table of Contents

1. Methods
2. Syntheses and Characterizations of 1 and 2
3. Supporting Figures and Tables

1. Methods

General methods

All the starting materials were obtained from Adamas or BaoMan Inc. (Shanghai). Commercially available reagents were used without further purification, unless noted otherwise. All chemicals were reagent grade or better. Recombinant intestinal alkaline phosphatase (ALP) was obtained from BaoMan Inc. (Shanghai) (one unit (U) is the enzyme activity that cleaves 1 μmol of the standard substrate per minute at 37 °C). Recombinant epidermal growth factor receptor (EGFR) was kindly supplied by Qingsong Liu's lab at the High Magnetic Field Laboratory. The electrospray ionization time-of-flight mass (ESI-TOF-MS) spectra were obtained on an Exactive Plus (Thermo Fisher Scientific, CA, USA) mass spectrometer. HPLC analyses were performed on an Agilent 1200 HPLC system equipped with a G1322A pump and in-line diode array UV detector using an Agilent Zorbax 300SB - C18 RP column with CH_3CN (0.1% of trifluoroacetic acid (TFA)) and water (0.1% of TFA) as the eluent. ^1H NMR spectra were obtained on a Bruker AV-300 MHz spectrometer. UV-vis absorption spectra were recorded on a Perkin-Elmer lambda 25 spectrophotometer. Cryo transmission electron microscopy (cryo-TEM) images were obtained on a Tecnai F20 transmission electron microscope from FEI Company, operating at 200 kV.

Liquid-Phase Scanning Tunneling Microscopy (L-STM)

As shown in Figure S1 below, the homebuilt L-STM in this work includes four key components: ultra-compact scan head, probe tip, sample pool, and the graphite surface (from top to down). The ultra-compact scan head was pushed by a high speed GeckoDrive piezo motor. The probe tip was obtained by mechanical shearing Pt/Ir wire (Purity: 90%: 10%, diameter: 0.25 mm, annealed, from Alfa Aesar), the angle between probe and scissor boundary tends to be 15 degree. To work in aqueous environment, the probe tip must be coated with suitable insulating material to avoid the generation of leakage current. Particularly, the probe tip was coated with poly methyl styrene at 180 °C, which minimizes the leakage current to lower than 20 pA. The sample pool is composed of an O-ring seal, the Teflon cell and a titanium plate, which are fixed together by screws. The 12 \times 12 mm^2 highly oriented pyrolytic graphite (HOPG-2 GRADE, from SPI) was stuck on the surface of titanium plate. Notably, we wrote procedures in LabView ourselves to ensure the dedicate control of the probe tip.

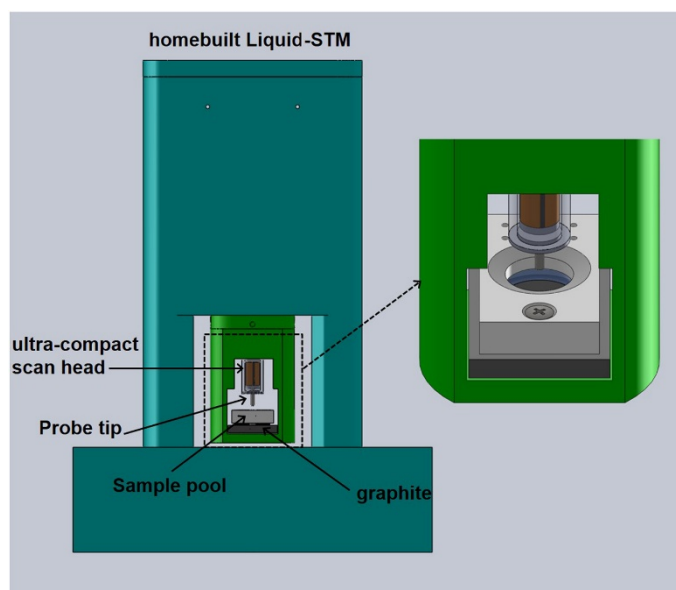


Figure S1. Assembled views of the overall stack for our homebuilt L-STM (left) and magnified image for the main part (right).

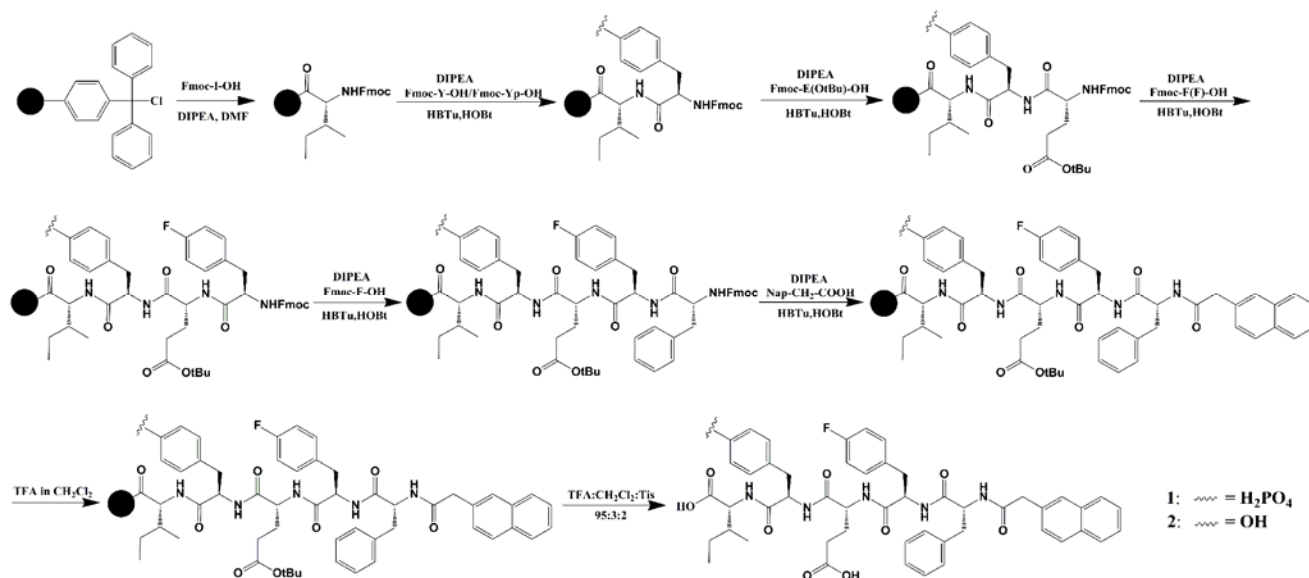
Imaging Mode for L-STM Observation

All our L-STM experiments are performed within three hours in air at 25 °C with an improved constant height mode. In principle, constant height imaging mode can be used to measure any samples with conductivity. We first steadily reduced the tip–surface distance by minishing the pre-set value of the tunneling current until a safe distance was obtained. Then we increased the pre-set value carefully during scanning process till a contrast of the target molecules could be seen in the images. In order to prevent the damages on the samples by probe tip, we added a line-based feed-back process in our constant height mode: within a certain line of scan, the scan height was not adjusted (remained constant), but when scanning the next line, the scan height was adjusted by calculating the average tunneling current of the previous line and attempting to maintain it to a pre-set constant. In this way, the supramolecular fiber would not be removed by the tip. During constant height imaging mode, the distance between the relative huge protein molecule and tip was smallest, thus the tunneling current at this point was the highest (up to 20 nA of protein-top surface in our images). However, the highest tunneling current on the fibers was much lower than 20 nA, about 5 nA, and the average tunneling current per line (which equals $I_{\text{pre-set}}$ in our manuscript) was about 1~4 nA.

2. Syntheses and Characterizations of 1 and 2

Preparation for compound Nap-Phe-Phe(F)-Glu-Tyr(H₂PO₃)-Ile-OH (**1**) and compound Nap-Phe-Phe(F)-Glu-Tyr-Ile-OH (**2**):

Scheme S1. The synthetic routes for **1** and **2**.



Syntheses of 1 and 2: Compound **1** or **2** was synthesized with solid phase peptide synthesis (SPPS), followed by the deprotection of tBu groups with dichloromethane (DCM, 300 μ L) and triisopropylsilane (TIPS, 200 μ L) in TFA (9.5 mL) for 3 h, purified with HPLC using water-acetonitrile added with 0.1% TFA as the eluent (from 6:4 to 2:8), and sent for high-resolution (HR) mass spectrum analysis.

¹H NMR of compound **1** (*d*₆-DMSO, 300 MHz, Figure S2) δ (ppm): 8.26 (d, *J* = 8.1 Hz, 1 H), 8.25 (d, *J* = 8.3 Hz, 1 H), 8.17 (d, *J* = 8.1 Hz, 1 H), 8.09 (d, *J* = 7.9 Hz, 1 H), 7.85 (d, *J* = 7.9 Hz, 1 H), 7.75 (s, 1 H), 7.72 (s, 1 H), 7.47-7.43 (m, 2 H), 7.41 (s, 1 H), 7.39 (s, 1 H), 7.23-7.13 (m, 10 H), 7.04-6.94 (m, 4 H), 4.61-4.48 (m, 3 H), 4.29 (m, 1 H), 4.18 (m, 1 H), 3.52 (m, 2 H), 2.89 (m, 2 H), 2.68 (m, 2 H), 2.21 (m, 2 H), 1.90-1.68 (m, 3 H), 1.44-1.13 (m, 2 H), 0.86-0.80 (m, 6 H). ¹³C NMR of **1** (75 MHz, *d*₆-DMSO, Figure S3) δ (ppm): ¹³C NMR (75 MHz, *d*₆-DMSO) δ 174.0, 172.7, 171.2, 170.9, 170.8, 170.6, 169.7, 159.3, 150.0, 150.0, 137.7, 133.9, 133.7, 133.0, 132.8, 131.7, 131.0, 130.9, 130.2, 129.2, 127.8, 127.5, 127.4, 127.3, 127.2, 126.1, 125.9, 125.4, 119.6, 119.6, 114.8, 114.5, 56.28, 53.63, 53.46, 51.66, 42.13, 37.42, 36.32, 29.96, 27.77, 24.58, 15.44, 11.19. ³¹P NMR (122 MHz, *d*₆-DMSO, Figure S4) δ (ppm): -6.21. MS: calculated for **1** (C₅₀H₅₅FN₅O₁₃P) [(M+H)⁺]: 984.3596; obsvd. HR-ESI-MS: *m/z* 984.3591 (Figure S5).

^1H NMR of compound **2** (d_6 -DMSO, 300 MHz, Figure S6) δ (ppm): 8.25 (d, $J = 8.5$ Hz, 1 H), 8.09 (d, $J = 8.0$ Hz, 1 H), 7.96 (d, $J = 8.0$ Hz, 1 H), 7.83 (d, $J = 8.0$ Hz, 1 H), 7.75 (s, 1 H), 7.72 (s, 1 H), 7.57 (s, 1 H), 7.53 (s, 1 H), 7.51 (s, 1 H), 7.47-7.43 (m, 2 H), 7.41 (s, 1 H), 7.39 (s, 1 H), 7.18-7.10 (m, 7 H), 7.04-6.92 (m, 4 H), 6.62 (s, 1 H), 6.60 (s, 1 H), 4.66-4.50 (m, 3 H), 4.35-4.27 (m, 1 H), 4.22-4.16 (m, 1 H), 3.62-3.42 (m, 2 H), 3.09-2.68 (m, 6 H), 2.22 (m, 2 H), 1.90-1.68 (m, 3 H), 1.44-1.15 (m, 2 H), 0.86-0.80 (m, 6 H). ^{13}C NMR of **2** (75 MHz, d_6 -DMSO, Figure S7) δ (ppm): 173.1, 171.9, 170.2, 169.7, 169.6, 168.8, 161.6, 158.4, 154.8, 136.8, 132.9, 132.8, 132.7, 131.9, 130.7, 130.1, 130.0, 129.2, 128.3, 126.9, 126.6, 126.5, 126.4, 126.3, 125.2, 125.0, 124.5, 113.9, 113.6, 77.57, 55.32, 52.73, 50.74, 41.23, 36.50, 35.55, 35.45, 29.06, 26.94, 23.69, 14.53, 10.30. MS: calculated for **2** ($\text{C}_{50}\text{H}_{54}\text{FN}_5\text{O}_{10}$) $[(\text{M}+\text{H})^+]$: 904.3933; obsvd. HR-ESI-MS: m/z 904.3922 (Figure S8).

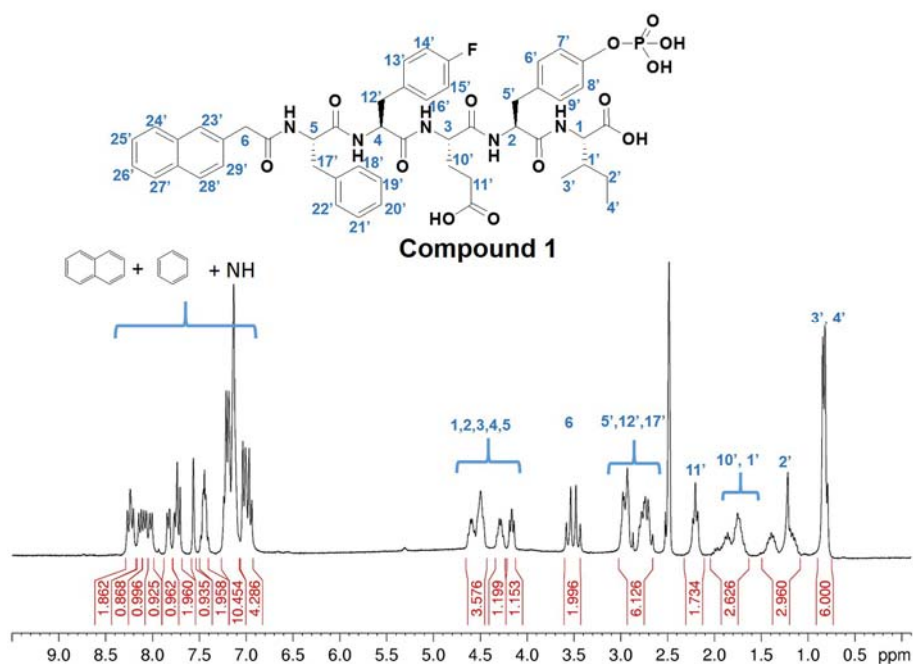


Figure S2. ^1H NMR spectrum of compound **1** in d_6 -DMSO.

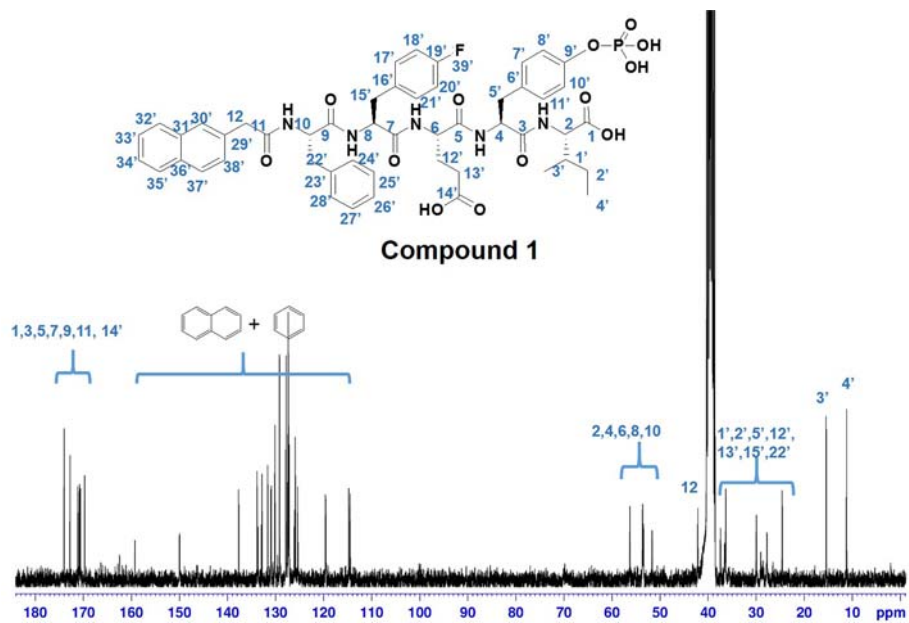


Figure S3. ^{13}C NMR spectrum of compound **1** in d_6 -DMSO.

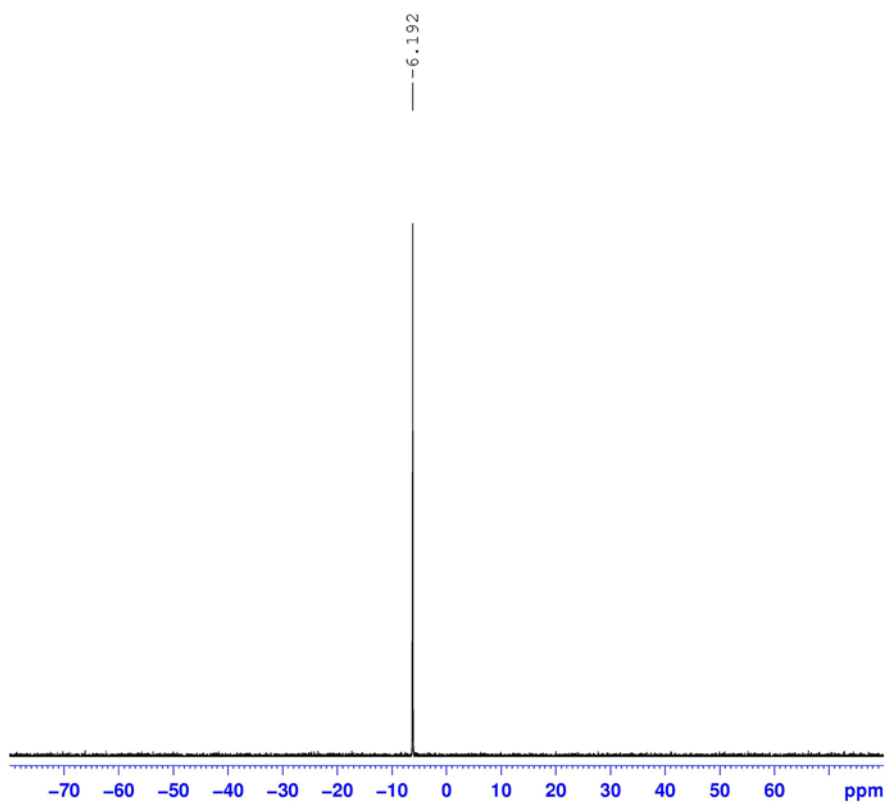


Figure S4. ^{31}P NMR spectrum of compound **1** in d_6 -DMSO.

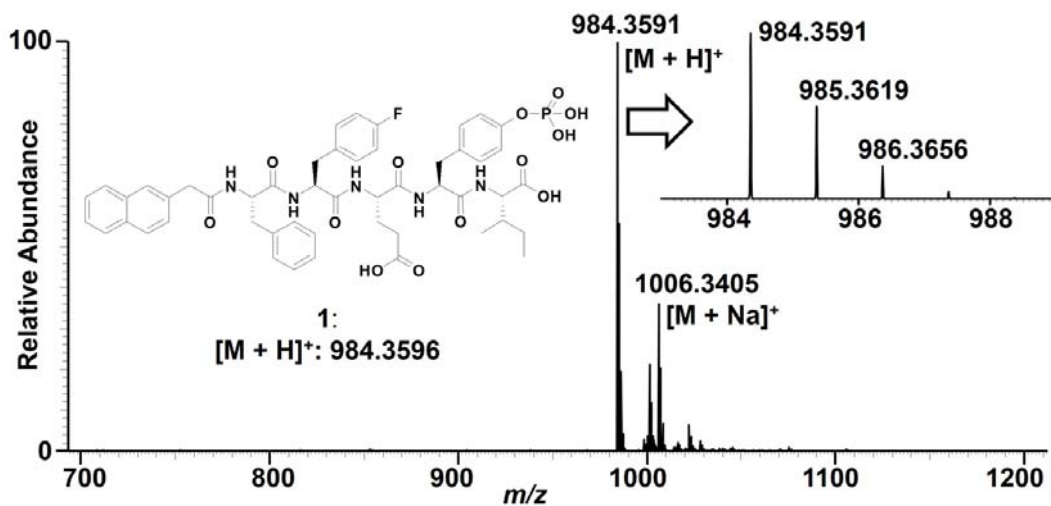


Figure S5. HR-ESI-MS spectrum of 1.

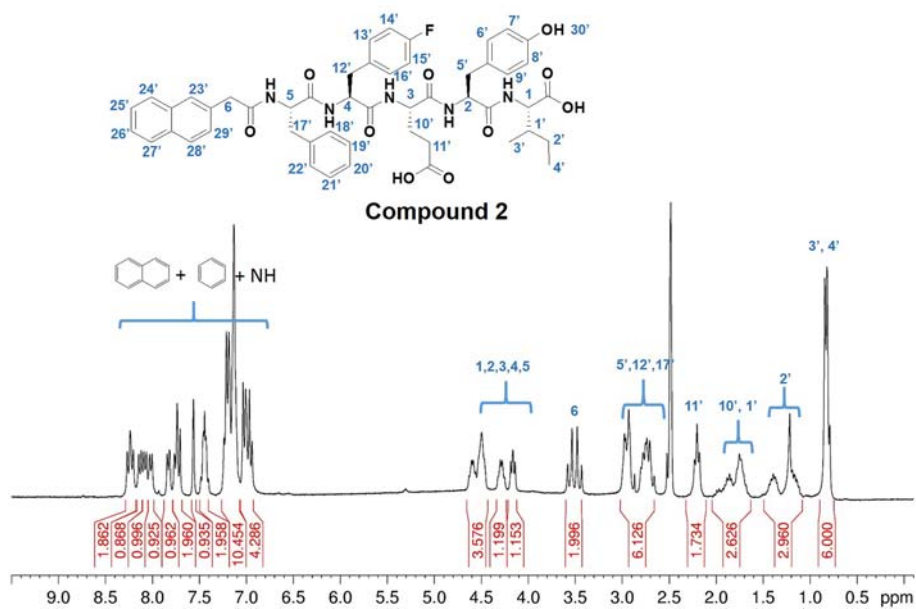


Figure S6. ^1H NMR spectrum of compound 2 in d_6 -DMSO.

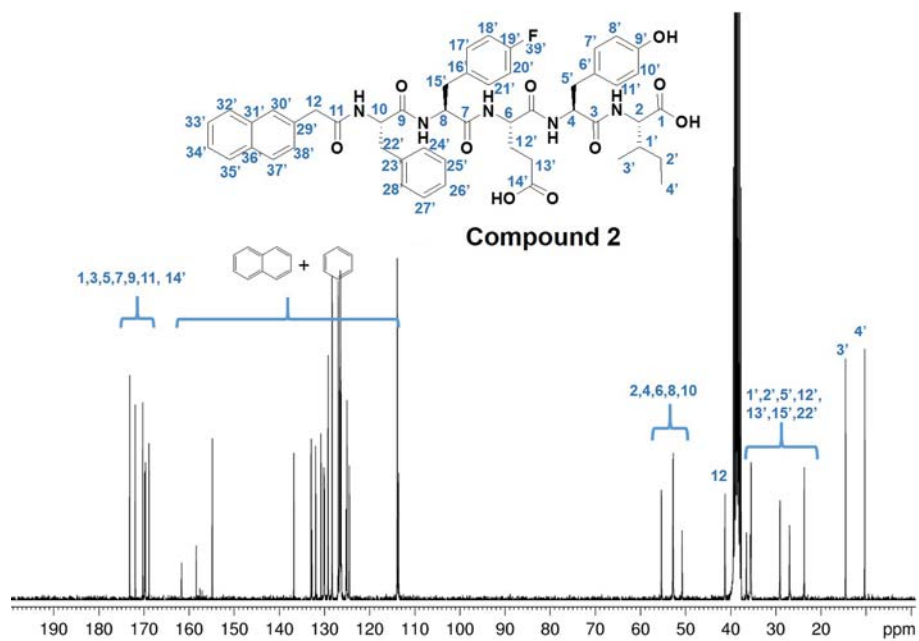


Figure S7. ^{13}C NMR spectrum of compound **1** in d_6 -DMSO.

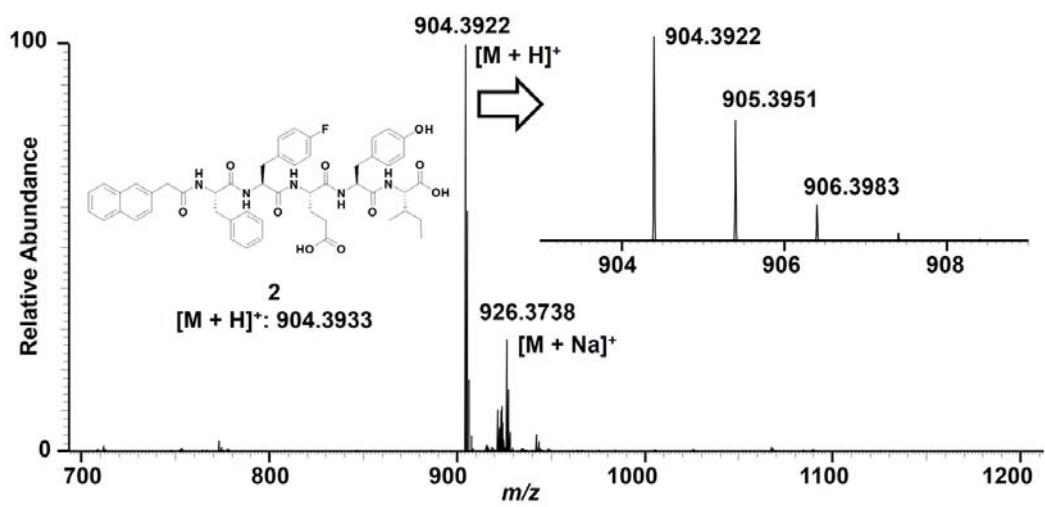


Figure S8. HR-ESI-MS spectrum of **2**.

3. Supporting Figures and Tables

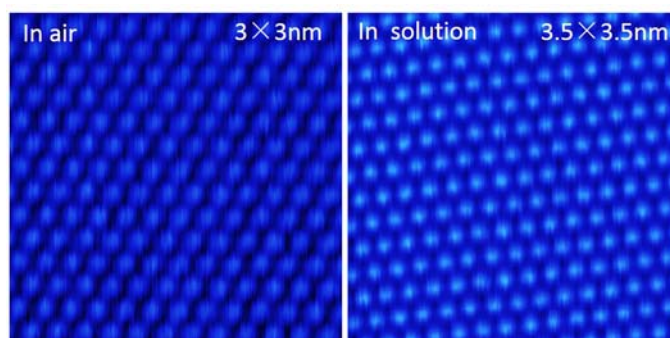


Figure S9. High-resolution STM images of the graphite surface in air (left) or in solution (right).

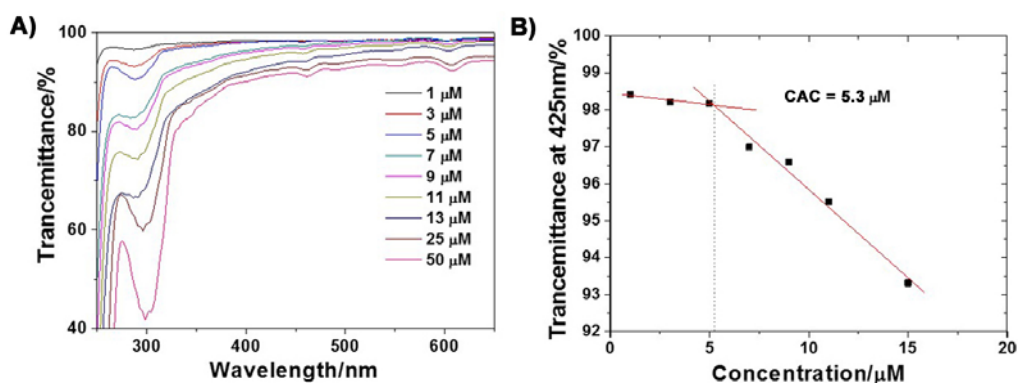


Figure S10. (A) Transmittance spectra of hydrogelator **2** at different concentrations. (B) Plotted transmittance-concentration curve of **2** at 425 nm for the determination of its critical aggregation concentration (CAC).

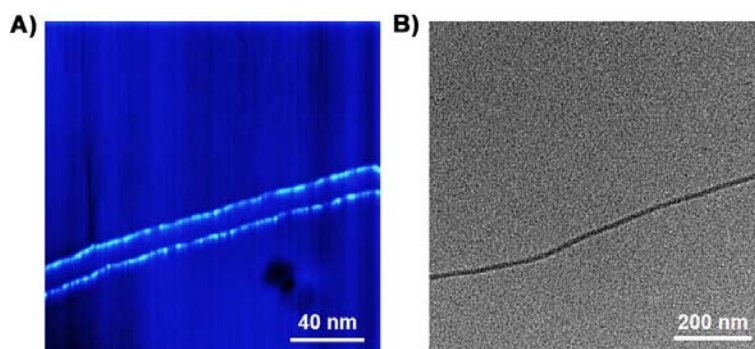


Figure S11. The L-STM image of nanofibers of **2** deposited on the graphite surface (A) and the corresponding TEM image under the same condition (B).

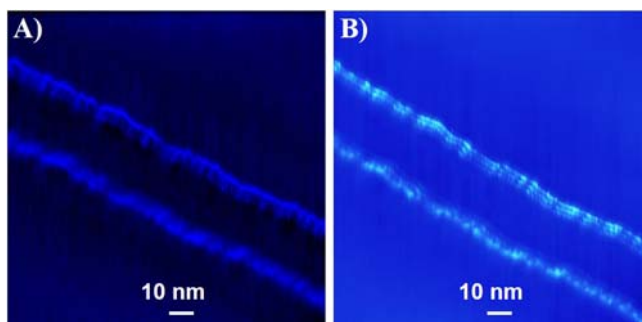


Figure S12. L-STM images of supramolecular nanofibers deposited on the graphite surface obtained under constant current mode (A), and line-based constant current mode with the same probe tip (B). (A) and (B) are performed in the same scanning region. Measurement conditions: bias voltage = +100 mV, tunneling current $I = 2$ nA, scan rates: 133.3 s/image for (A), and 26.7 s/image for (B).

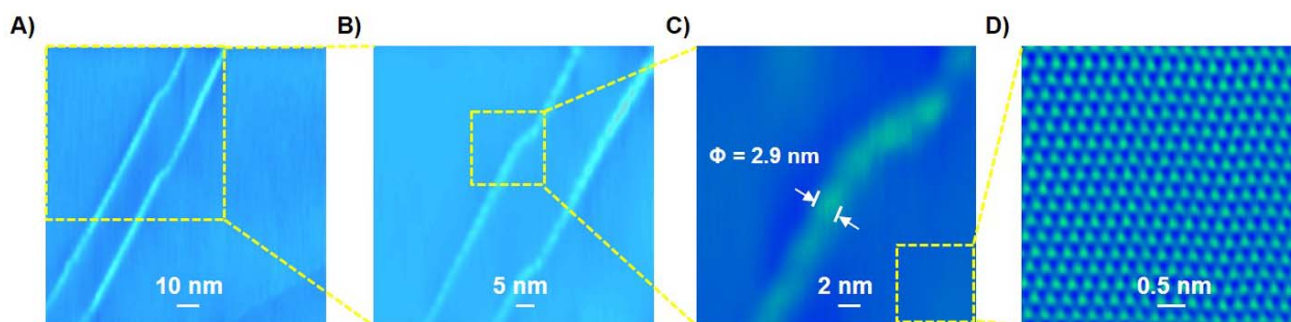


Figure S13. (A) L-STM image of nanofibers of **2** deposited on the graphite surface. (B) A zoom-in scan of the square enclosed region in A. (C) A zoom-in scan of the square enclosed region in B. (D) A zoom-in scan of the square enclosed region in C. Measurement conditions: bias voltage = +100 mV, tunneling current $I_{\text{pre-set}} = 2$ nA, scan rate = 26.7 s/image, image sizes: 125×125 nm (A), 75×75 nm (B), 25×25 nm (C), and 5×5 nm (D).

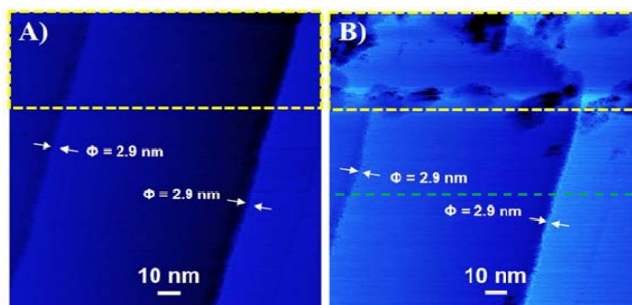


Figure S14. (A) L-STM image of nanofibers of **2** deposited on the graphite surface under constant current mode (raw data). (B) L-STM image of the same nanofibers with marked region in A scanned at very low gap distance so as to use the tip to displace the fiber. Measurement conditions: bias voltage = +100 mV, tunneling current $I = 1$ nA, scan rate = 133.3 s/image, scan range: 140×140 nm.

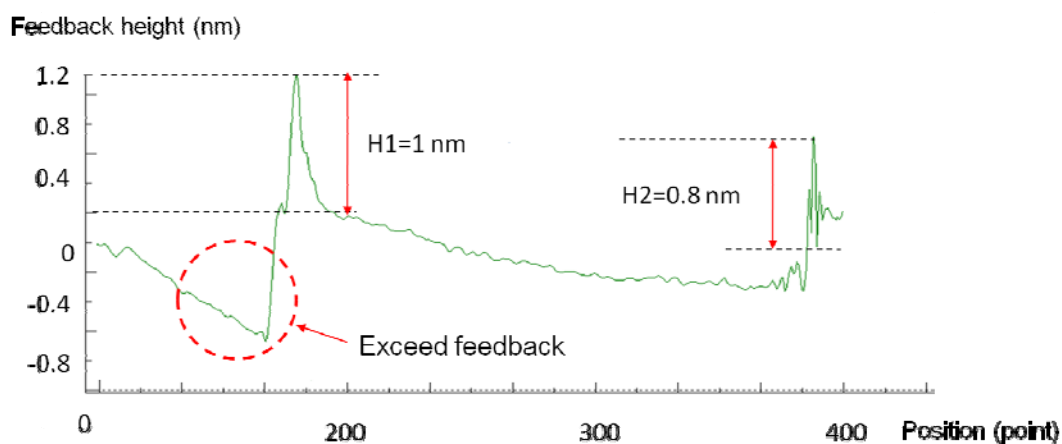


Figure S15. Height profile of the green dotted line-marked region in Figure S14.

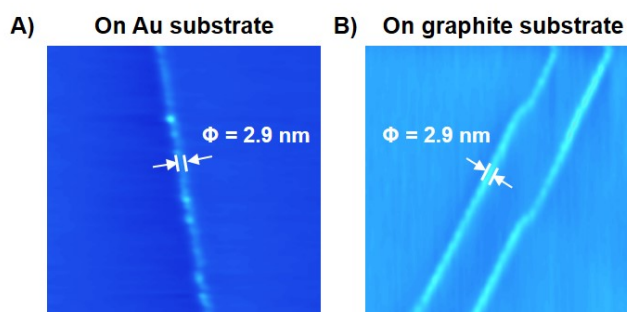


Figure S16. The L-STM images of nanofibers of **2** deposited on Au (A) or graphite (B) substrate. Measurement conditions: image size = 90×90 nm, bias voltage = +100 mV, tunneling current $I_{\text{pre-set}}$: 3 nA for A and 2 nA for B, scan rate = 26.7 s/image.

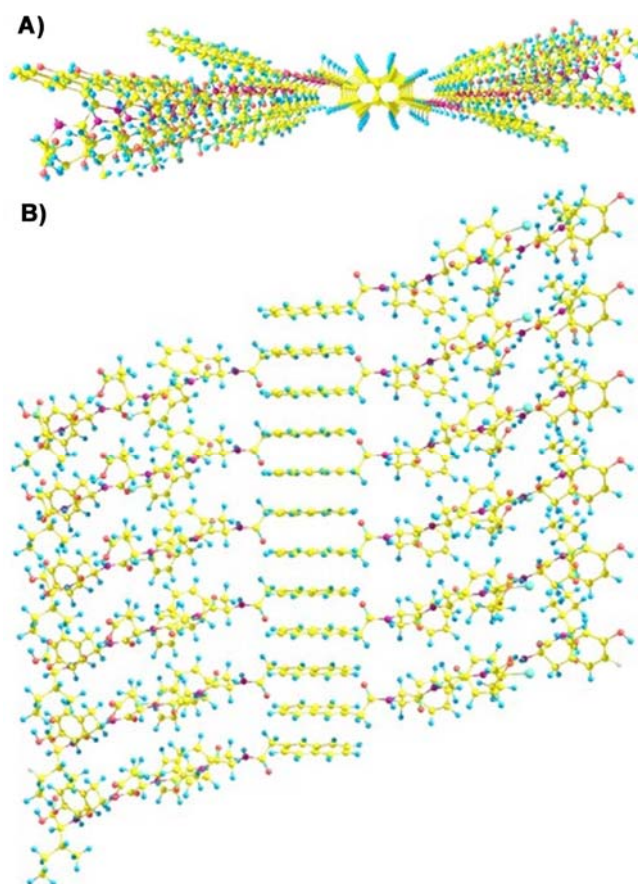


Figure S17. Top (A) and side (B) views of proposed molecular arrangement of **2** in the nanofibers.

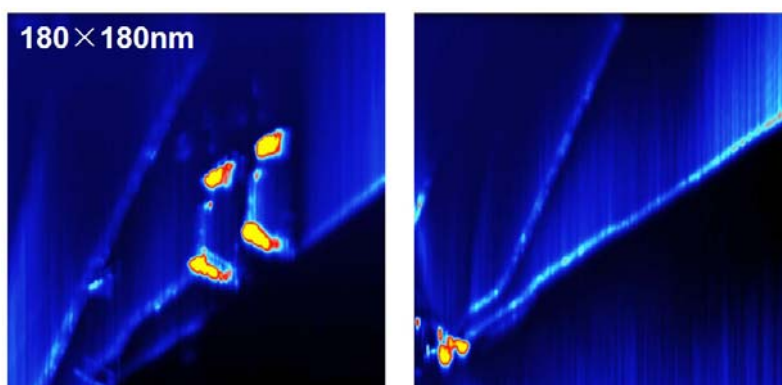


Figure S18. L-STM images of enzyme ALP in the vicinity of the nanofibers.

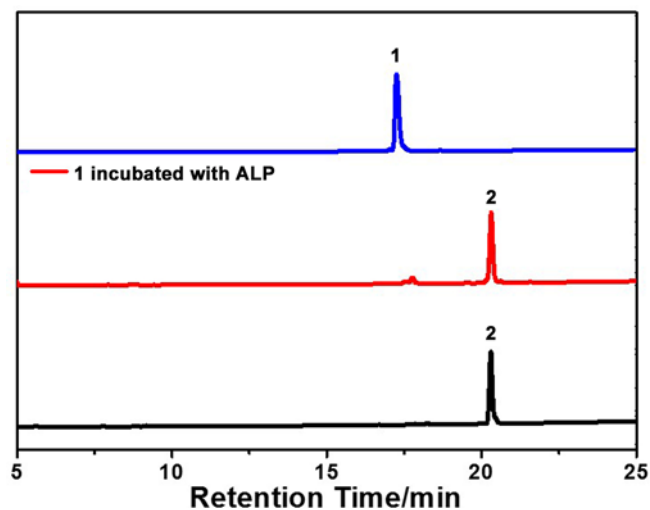


Figure S19. HPLC traces for precursor **1** at 200 μM (blue), 200 μM **1** incubated with ALP for 1 h (red), and hydrogelator **2** (black), respectively. Wavelength for detection: 268 nm.

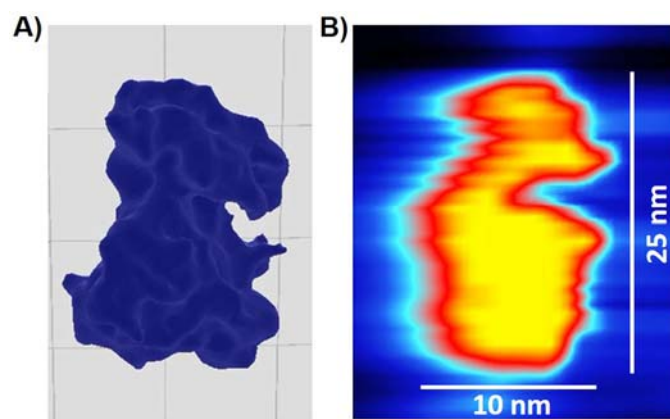


Figure S20. (A) Simulative model for EGFR based on its crystal structure. (B) Observed L-STM image of EGFR in working buffer in this work.

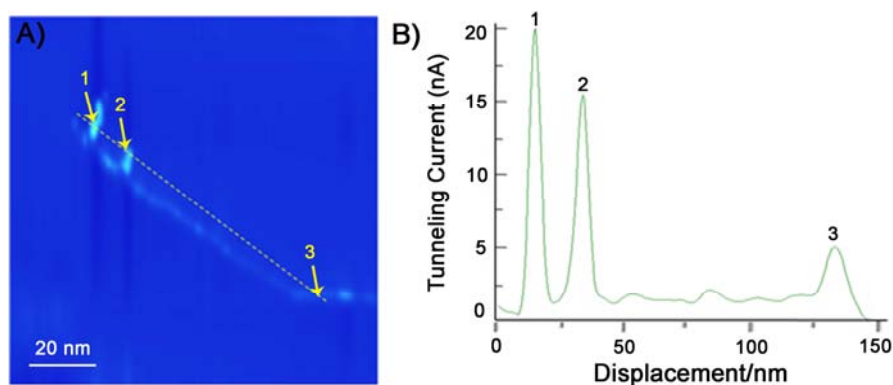


Figure S21. (A) L-STM image of EGFR-instructed molecular disassembly of **2** from the pre-prepared nanofibers. Tunneling current $I_{\text{pre-set}}$: 2.5 nA; Bias voltage: 0.1 V. (B) Tunneling current curve along the dotted yellow line in A. Peaks 1 and 2 in the curve which are higher than 15 nA correspond to the topsurfaces of the protein, and peak 3 with a value of 5 nA corresponds to the topsurface of the fiber.

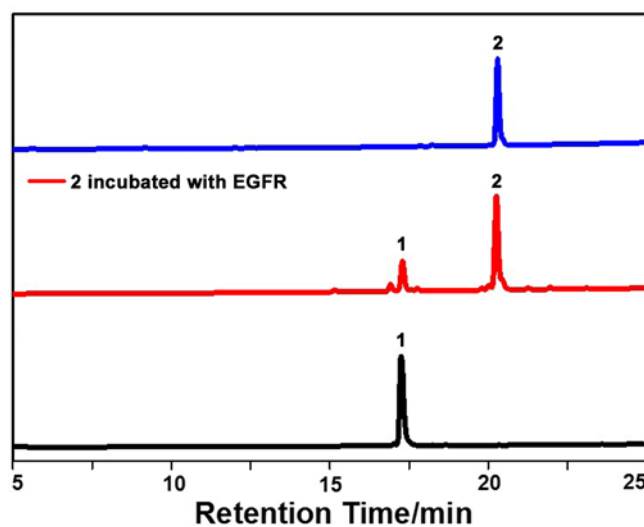


Figure S22. HPLC traces for hydrogelator **2** at 200 μM (blue), 200 μM **2** incubated with EGFR for 1 h (red), and precursor **1** (black), respectively. Wavelength for detection: 268 nm.

Table S1. HPLC condition for the purification of compound **1** and **2**.

Time (minute)	Flow (ml/min.)	H ₂ O %	CH ₃ CN %
0	3.0	60	40
3	3.0	60	40
35	3.0	20	80
37	3.0	20	80
38	3.0	60	40
40	3.0	60	40

Table S2. HPLC condition for the analyses in Figure S19 and Figure S22.

Time (minute)	Flow (ml/min.)	H ₂ O %	CH ₃ CN %
0	3.0	70	30
3	3.0	70	30
35	3.0	10	90
37	3.0	10	90
38	3.0	70	30
40	3.0	70	30